J Eng Math (2007) 59:83–97
DOI 10.1007/s10665-006-9072-z

ORIGINAL PAPER

Electroelastic response of a flat annular crack in a piezoelectric fiber surrounded by an elastic medium

Y. Shindo · S. Lin · F. Narita

Received: 8 December 2005 / Accepted: 3 July 2006 / Published online: 14 November 2006

Abstract Following the theory of linear piezoelectricity, the electroelastic problem of a flat annular crack in a piezoelectric fiber embedded in an elastic medium is considered. Fourier and Hankel transform techniques are employed to formulate the mixed-boundary-value problem as a singular integral equation. The stress-intensity factor, energy-release rate and energy-density factor are computed for some piezoelectric composites, and the influence of applied electric fields on the normalized values is displayed graphically.

Keywords Elasticity · Energy release rate · Integral transforms · Piezocomposites · Smart material systems

1 Introduction

Piezoelectric fiber composites are an important branch of modern engineering materials, with wide applications in sensors and actuators [1–3]. In the last decades, electric fracture behavior of piezoelectric materials has been the topic of many discussions [4–6]. In theoretical studies of piezoelectric crack problems, there are two commonly used electrical boundary conditions imposed across the crack surface, (1) the permeable crack model, and (2) the impermeable crack model. Recently, Shindo et al. [7] employed a finite-element analysis of piezoelectric composite double-torsion (DT) specimens for various electric fields to calculate the energy release rate for permeable and impermeable crack models, and conducted DT tests to verify theoretical predictions on the influence of an applied electric field on piezoelectric fracture behavior. They concluded that the impermeable boundary conditions should not be used in engineering practice because the criteria are unreliable and may yield misleading results. Analyses of cracked piezoelectric ceramics [8, 9] and composites [10, 11] also indicated that a negative energy release rate is produced for the impermeable crack model. Narita et al. [12] made finite-element analyses of the single-edge precracked-beam (SEPB) and indentation fracture (IF) tests on the piezoelectric ceramics based on the use of permeable and impermeable boundary conditions. They, for example, found that for a given residual force derived from the indentation plastic zone, the positive electric fields decrease the energy release rate

Y. Shindo (✉) · S. Lin · F. Narita
Department of Materials Processing, Graduate School of Engineering, Tohoku University,
Aoba-yama 6-6-02, Sendai 980-8579, Japan
e-mail: shindo@material.tohoku.ac.jp

at maximum depth point of the permeable crack, while negative electric fields have the opposite effect. The increase in the crack length with increasing positive electric field is attributed to an increase of the energy release rate with increasing positive electric field.

The geometry of internal flat annular cracks is of practical importance in electroelastic field-analysis, since it represents an idealization of the banana-shaped cracks that are inherent in many piezoelectric ceramics. This paper considers the mode I problem for a long piezoelectric fiber with a flat annular crack surrounded by an elastic matrix. Fourier- and Hankel-transform methods are used to formulate the electroelastic problem, in terms of a singular integral equation. Numerical results for the stress-intensity factor, energy-release rate and energy-density factor are displayed graphically and discussed in detail.

2 Problem statement and basic equations

A piezoelectric fiber of radius b and finite length with a flat annular crack is embedded in an elastic matrix having Young's modulus E and Poisson's ratio ν, as shown in Fig. 1. The problem will be formulated using a cylindrical coordinate system (r, θ, z), where the longitudinal axis and the poling axis of the fiber coincide with the z-axis. The crack is assumed to lie in a plane normal to the z-axis and occupies the region, $z = 0, c < r < a$, where c and a are the inner and outer radii of the flat annular crack, respectively. The piezoelectric fiber is transversely isotropic with hexagonal symmetry; it is subjected to a far-field normal strain $\varepsilon_{zz} = \varepsilon_\infty$ and electric field $E_z = E_\infty$ (normal stress $\sigma_{zz} = \sigma_\infty$). Quantities in the neighboring elastic matrix will subsequently be designated by a superscript E.

The equations of force and charge equilibriums without body force and internal charge are

$$\left.\begin{aligned} &\sigma_{rr,r} + \sigma_{zr,z} + \tfrac{\sigma_{rr}-\sigma_{\theta\theta}}{r} = 0, \\ &\sigma_{zr,r} + \sigma_{zz,z} + \tfrac{\sigma_{zr}}{r} = 0, \qquad 0 \le r < b, \end{aligned}\right\} \tag{1}$$

$$D_{r,r} + \frac{D_r}{r} + D_{z,z} = 0, \quad 0 \le r < b, \tag{2}$$

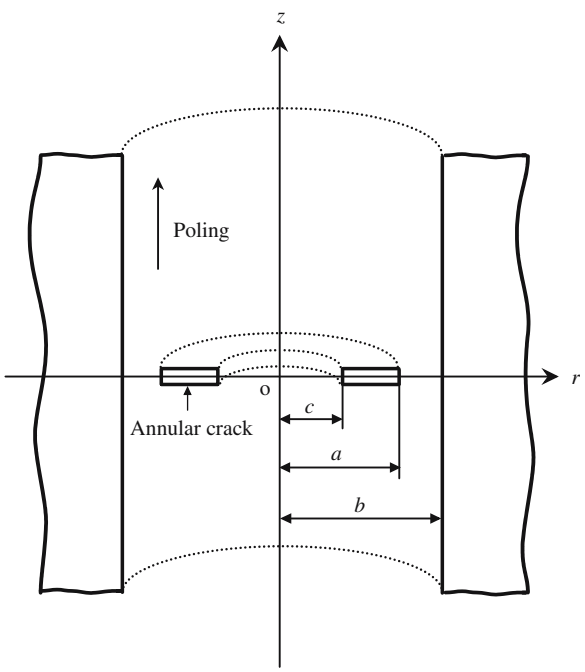

Fig. 1 Geometry of a piezoelectric fiber with a flat annular crack embedded in an elastic matrix

and

$$\left.\begin{aligned}\sigma^E_{rr,r}+\sigma^E_{zr,z}+\frac{\sigma^E_{rr}-\sigma^E_{\theta\theta}}{r}=0,\\ \sigma^E_{zr,r}+\sigma^E_{zz,z}+\frac{\sigma^E_{zr}}{r}=0,\quad r>b.\end{aligned}\right\} \tag{3}$$

The constitutive equations for the piezoelectric fiber and elastic matrix can be written as [13]

$$\left.\begin{aligned}\sigma_{rr}&=c_{11}u_{r,r}+c_{12}\frac{u_r}{r}+c_{13}u_{z,z}-e_{31}E_z,\\ \sigma_{\theta\theta}&=c_{12}u_{r,r}+c_{11}\frac{u_r}{r}+c_{13}u_{z,z}-e_{31}E_z,\\ \sigma_{zz}&=c_{13}u_{r,r}+c_{13}\frac{u_r}{r}+c_{33}u_{z,z}-e_{33}E_z,\\ \sigma_{zr}&=c_{44}(u_{r,z}+u_{z,r})-e_{15}E_r,\end{aligned}\right\} \tag{4}$$

$$\left.\begin{aligned}D_r&=e_{15}(u_{r,z}+u_{z,r})+\epsilon_{11}E_r,\\ D_z&=e_{31}\left(u_{r,r}+\frac{u_r}{r}\right)+e_{33}u_{z,z}+\epsilon_{33}E_z,\end{aligned}\right\} \tag{5}$$

$$\left.\begin{aligned}\sigma^E_{rr}&=(2\mu+\lambda)u^E_{r,r}+\lambda\left(\frac{u^E_r}{r}+u^E_{z,z}\right),\\ \sigma^E_{\theta\theta}&=\lambda u^E_{r,r}+(2\mu+\lambda)\frac{u^E_r}{r}+\lambda u^E_{z,z},\\ \sigma^E_{zz}&=\lambda\left(u^E_{r,r}+\frac{u^E_r}{r}\right)+(2\mu+\lambda)u^E_{z,z},\\ \sigma^E_{zr}&=\mu(u^E_{r,z}+u^E_{z,r}),\end{aligned}\right\} \tag{6}$$

where $\sigma_{rr},\sigma_{\theta\theta},\sigma_{zz},\ \sigma_{zr},\sigma^E_{rr},\sigma^E_{\theta\theta},\sigma^E_{zz},\sigma^E_{zr}$ are the components of the stress tensor; D_r and D_z the components of electric displacement vector; u_r,u_z,u^E_r and u^E_z the components of displacement vectors; E_r and E_z the components of electric-field vector; $c_{11},c_{12},c_{13},c_{33},c_{44}$ the elastic moduli measured in a constant electric field; $\epsilon_{11},\epsilon_{33}$ the dielectric permittivities measured at constant strain; e_{15},e_{31},e_{33} the piezoelectric constants; λ=$2G\nu/(1-2\nu)$ and $\mu=G$ the Lamé constants of the elastic matrix; and G=$E/2(1+\nu)$ the modulus of rigidity. A comma implies partial differentiation with respect to the coordinates. The electric field components are related to the electric potential $\phi(r,z)$ by

$$E_r=-\phi_{,r},\quad E_z=-\phi_{,z}. \tag{7}$$

By substituting from (4) and (5) in (1) and (2) together with (7), we can write the governing equations for the piezoelectric fiber as

$$\left.\begin{aligned}&c_{11}\left(u_{r,rr}+\frac{u_{r,r}}{r}-\frac{u_r}{r^2}\right)+c_{44}u_{r,zz}+(c_{13}+c_{44})u_{z,rz}+(e_{31}+e_{15})\phi_{,rz}=0,\\ &(c_{13}+c_{44})\left(u_{r,rz}+\frac{u_{r,z}}{r}\right)+c_{33}u_{z,zz}+c_{44}\left(u_{z,rr}+\frac{u_{z,r}}{r}\right)+e_{15}\left(\phi_{,rr}+\frac{\phi_{,r}}{r}\right)+e_{33}\phi_{,zz}=0,\quad 0\le r<b,\end{aligned}\right\} \tag{8}$$

$$(e_{31}+e_{15})\left(u_{r,rz}+\frac{u_{r,z}}{r}\right)+e_{15}\left(u_{z,rr}+\frac{u_{z,r}}{r}\right)+e_{33}u_{z,zz}-\epsilon_{11}\left(\phi_{,rr}+\frac{\phi_{,r}}{r}\right)-\epsilon_{33}\phi_{,zz}=0,\quad 0\le r<b. \tag{9}$$

Similarly, we obtain

$$\left.\begin{aligned}&(2\mu+\lambda)\left(u^E_{r,rr}+\frac{u^E_{r,r}}{r}-\frac{u^E_r}{r^2}\right)+\mu u^E_{r,zz}+(\mu+\lambda)u^E_{z,rz}=0,\\&(\mu+\lambda)\left(u^E_{r,rz}+\frac{u^E_{r,z}}{r}\right)+(2\mu+\lambda)u^E_{z,zz}+\mu\left(u^E_{z,rr}+\frac{u^E_{z,r}}{r}\right)=0,\quad r>b.\end{aligned}\right\} \tag{10}$$

In a vacuum, the constitutive equations (5) and the governing equation (9) become

$$D_r=\epsilon_0 E_r,\quad D_z=\epsilon_0 E_z, \tag{11}$$

$$\phi_{,rr}+\frac{\phi_{,r}}{r}+\phi_{,zz}=0, \tag{12}$$

where $\epsilon_0=8.85\times10^{-12}$ C/Vm is the electric permittivity of the vacuum.

It is sufficient to consider the problem for the semi-infinite region $z\ge 0, 0\le r<\infty, 0\le\theta\le 2\pi$ only. The crack is traction-free and on its surface the normal component of the electric displacement and the tangential component of the electric field are continuous. Also, the geometry and/or the fields are symmetry. Thus

$$\begin{aligned}&\sigma_{zr}(r,0)=0\quad(0\le r\le b),\\&\sigma^E_{zr}(r,0)=0\quad(b\le r<\infty),\end{aligned} \tag{13}$$

$$\begin{aligned}&\sigma_{zz}(r,0)=0\quad(c<r<a),\\&u_z(r,0)=0\quad(0\le r\le c,\ \ a\le r\le b),\\&u^E_z(r,0)=0\quad(b\le r<\infty),\end{aligned} \tag{14}$$

$$\begin{aligned}&E_r(r,0)=E^c_r(r,0)\ (c<r<a),\\&\phi(r,0)=0\qquad\quad(0\le r\le c,\ \ a\le r\le b),\end{aligned} \tag{15}$$

$$D_z(r,0)=D^c_z(r,0)\quad(c<r<a), \tag{16}$$

where the superscript c denotes the electric field quantity in the void inside the crack. At $r=b$ the continuities of displacements and stresses require that

$$u_r(b,z)=u^E_r(b,z), \tag{17}$$

$$u_z(b,z)=u^E_z(b,z), \tag{18}$$

$$\sigma_{rr}(b,z)=\sigma^E_{rr}(b,z), \tag{19}$$

$$\sigma_{rz}(b,z)=\sigma^E_{rz}(b,z). \tag{20}$$

In electrostatics, at a surface separating two dielectric bodies, the normal component of the electric displacement and the tangential component of the electric field are continuous. However, when one of the bodies is an elastic body, these two conditions can be approximated simply by one, namely that the normal component of the electric displacement vanishes at the interface. So the electrical boundary condition at $r=b$ is (see [12])

$$D_r(b,z)=0. \tag{21}$$

This assumption of impermeability is based on the fact that there ia a very large difference between the dielectric constants of the piezoelectric fiber and the elastic matrix. This does not mean that the elastic matrix is grounded, i.e., $\phi(b,z) \neq 0$. The loading conditions at infinity are

$$\begin{aligned} &\varepsilon_{zz}(r,z) = \varepsilon_\infty, \quad E_z(r,z) = E_\infty \quad (0 \le r \le b, \ \ z \to \infty), \\ &\varepsilon^E_{zz}(r,z) = \varepsilon_\infty \quad (b \le r < \infty, \ \ z \to \infty). \end{aligned} \tag{22}$$

Equations 15 and 16 are the permeability boundary conditions. The electric potential is uniformly zero on the symmetry planes inside the crack and ahead of the crack, so the boundary conditions of (15) reduce to $\phi(r,0) = 0 \ \ (0 \le r \le b)$. The electric-field intensity $E^c_r(r,0)$ is equal to zero, and the electric displacement $D^c_z(r,0)$ is determined precisely.

On the other hand, when a spherical or a spheroidal defect problem in a piezoelectric fiber is analyzed, the impermeability condition is a good approximation. The electroelastic fields around a defect for the impermeable crack model, however, are quite different from those for the permeable-crack model when the defect becomes a sharp crack. Therefore, the crack problem should not be solved with the impermeability condition [12]. Of course, the impermeable flat annular-crack model, $D_z(r,0) = 0 \ (c < r < a)$, has not been treated yet.

By applying the loading conditions (22), the far-field normal stresses σ_∞ and σ^E_∞ are expressed as

$$\sigma_\infty = \sigma_0 - e_1 E_\infty, \quad \sigma^E_\infty = c_1(\sigma_\infty + e_1 E_\infty), \tag{23}$$

where

$$\begin{aligned} c_1 &= \frac{2\mu(1+\nu)(c_{11}+c_{12}-\lambda)}{2c_{13}(\lambda\nu - c_{13}) + c_{33}(c_{11}+c_{12}-\lambda)}, \\ e_1 &= e_{33} + \frac{2c_{13}e_{31}}{\lambda - c_{11} - c_{12}}, \end{aligned} \tag{24}$$

and

$$\sigma_0 = \left\{ c_{33} - \frac{2c_{13}(c_{13} - \lambda\nu)}{c_{11} + c_{12} - \lambda} \right\} \varepsilon_\infty. \tag{25}$$

Note that σ_0 is a uniform normal stress for a closed-circuit condition with the potential forced to remain zero (grounded), and depends only on the strain at infinity. When a uniform strain ε_∞ is applied and fixed at infinity, the stress σ_0 will be uniform. When the stress σ_∞ is applied and fixed at infinity, σ_∞ is left unchanged and the strain ε_∞ depends on E_∞.

3 Solution procedure

Let the solutions of (8)–(10) be of the form

$$\begin{aligned} u_r(r,z) &= \frac{2}{\pi}\sum_{j=1}^{3}\int_0^\infty [a_j A_j(\alpha)\exp(-\gamma_j\alpha z)J_1(\alpha r) + a_j' B_j(\alpha) I_1(\gamma_j'\alpha r)\cos(\alpha z)]\,\mathrm{d}\alpha + a_\infty r, \\ u_z(r,z) &= \frac{2}{\pi}\sum_{j=1}^{3}\int_0^\infty \left[\frac{1}{\gamma_j}A_j(\alpha)\exp(-\gamma_j\alpha z)J_0(\alpha r) + \frac{1}{\gamma_j'}B_j(\alpha)I_0(\gamma_j'\alpha r)\sin(\alpha z)\right]\mathrm{d}\alpha + b_\infty z, \\ &\quad 0 \le r < b, \end{aligned} \tag{26}$$

$$\begin{aligned} \phi(r,z) &= \frac{2}{\pi}\sum_{j=1}^{3}\int_0^\infty \left[-\frac{b_j}{\gamma_j}A_j(\alpha)\exp(-\gamma_j\alpha z)J_0(\alpha r) + \frac{b_j'}{\gamma_j'}B_j(\alpha)I_0(\gamma_j'\alpha r)\sin(\alpha z)\right]\mathrm{d}\alpha - c_\infty z, \\ &\quad 0 \le r < b, \end{aligned} \tag{27}$$

$$u_r^E(r,z) = \frac{2}{\pi}\int_0^\infty \{-K_1(\alpha r)B_4(\alpha) + [4(1-\nu)K_1(\alpha r) + \alpha r K_0(\alpha r)]B_5(\alpha)\}\cos(\alpha z)\,\mathrm{d}\alpha + a_\infty b + d_\infty(r-b),$$
$$u_z^E(r,z) = \frac{2}{\pi}\int_0^\infty [-K_0(\alpha r)B_4(\alpha) + \alpha r K_1(\alpha r)B_5(\alpha)]\sin(\alpha z)\,\mathrm{d}\alpha + e_\infty z, \quad r > b, \tag{28}$$

where $A_j(\alpha)$ $(j = 1,2,3)$ and $B_j(\alpha)$ $(j = 1,\ldots,5)$ are the unknown functions to be solved, $J_0()$ and $J_1()$ are the zero- and first-order Bessel functions of the first kind, $I_0()$ and $I_1()$ are the zero- and first-order modified Bessel functions of the first kind, and $K_0()$ and $K_1()$ are the zero- and first-order modified Bessel functions of the second kind, respectively. Details of the derivation of (26)–(28) are given in Appendix 1. The real constants $a_\infty, b_\infty, c_\infty, d_\infty$ and e_∞ will be determined from the far-field loading conditions, and $\gamma_j^2, a_j, b_j, \gamma_j'^2, a_j', b_j'$ $(j = 1,2,3)$ are given in Appendix 1. Application of the Fourier transform to (12) yields

$$\phi^c(r,z) = \frac{2}{\pi}\int_0^\infty C(\alpha)\sinh(\alpha z)J_0(\alpha r)\,\mathrm{d}\alpha, \quad c < r < a, \tag{29}$$

where $C(\alpha)$ is also unknown. It can be shown that $\phi^c(r,0) = 0,\ c < r < a$.

By applying the far-field loading conditions, we obtain the constants $a_\infty, b_\infty, c_\infty, d_\infty$ and e_∞ as

$$a_\infty = \frac{1}{c_{11}+c_{12}-\lambda}\{(\lambda\nu - c_{13})\varepsilon_\infty + e_{31}E_\infty\}, \quad b_\infty = e_\infty = \varepsilon_\infty, \quad c_\infty = E_\infty, \quad d_\infty = -\nu\varepsilon_\infty. \tag{30}$$

The following relations between unknown functions are obtained from the boundary conditions of the first of Eqs. 13 and 15:

$$\frac{f_1}{\gamma_1}A_1(\alpha) + \frac{f_2}{\gamma_2}A_2(\alpha) + \frac{f_3}{\gamma_3}A_3(\alpha) = 0, \tag{31}$$
$$\frac{b_1}{\gamma_1}A_1(\alpha) + \frac{b_2}{\gamma_2}A_2(\alpha) + \frac{b_3}{\gamma_3}A_3(\alpha) = 0, \tag{32}$$

where

$$f_j = c_{44}(a_j\gamma_j^2 + 1) - e_{15}b_j \quad (j = 1,2,3). \tag{33}$$

Solving for $A_2(\alpha)$ and $A_3(\alpha)$ from (31) and (32), we see that

$$A_2(\alpha) = \frac{d_2}{d_1}A_1(\alpha), \tag{34}$$
$$A_3(\alpha) = \frac{d_3}{d_1}A_1(\alpha), \tag{35}$$

where

$$d_1 = \gamma_1(b_2f_3 - b_3f_2), \quad d_2 = \gamma_2(b_3f_1 - b_1f_3), \quad d_3 = \gamma_3(b_1f_2 - b_2f_1). \tag{36}$$

Introduce the new function $\psi(r), c < r < a$, by

$$u_{z,r}(r,0) = \frac{2}{\pi}\psi(r)\sum_{j=1}^{3}\frac{d_j}{\gamma_j}, \quad c < r < a. \tag{37}$$

Then, the second of Eq. 14 is satisfied if

$$\int_c^a \psi(t)\,\mathrm{d}t = 0. \tag{38}$$

Substituting the second of Eq. 26 in Eq. 37 and applying an inverse Hankel transform, we find that

$$A_1(\alpha) = -d_1\int_c^a t\psi(t)J_1(\alpha t)\,\mathrm{d}t. \tag{39}$$

The second of Eq. 13 and the third of Eq. 14 are automatically satisfied by the solutions in (26) and (28). By substituting from (26–28) in (17–21) together with in (4–7), using (34), (35), (39) and solving the resulting equations for $B_j(\alpha)$ $(j = 1, \ldots, 5)$ in terms of $\psi(t)$, we may write the unknowns $B_j(\alpha)$ $(j = 1, \ldots, 5)$ as

$$B_j(\alpha) = \frac{2}{\pi} \int_c^a t\psi(t) \sum_{i=1}^{5} \frac{P_i(\alpha, t) Q_{i,j}(\alpha)}{|\mathbf{C}(\alpha)|} \, \mathrm{d}t, \quad (j = 1, \ldots, 5), \tag{40}$$

where $P_i(\alpha, t)$, $Q_{i,j}(\alpha)$ and $|\mathbf{C}(\alpha)|$ are given in Appendix 2. Using the results, the stress $\sigma_{zz}(r, 0)$ takes the form

$$\sigma_{zz}(r, 0) = -\frac{2}{\pi} F \int_c^a \psi(t) \{R(r, t) + S(r, t)\} \, \mathrm{d}t, \quad c < r < a, \tag{41}$$

where

$$\begin{aligned} R(r, t) &= \frac{2}{\pi} \frac{t}{r^2 - t^2} E\left(\frac{r}{t}\right); \quad r < t, \\ &= \frac{2}{\pi} \left\{ \frac{r}{r^2 - t^2} E\left(\frac{t}{r}\right) - \frac{1}{r} K\left(\frac{t}{r}\right) \right\}; \quad r > t, \end{aligned} \tag{42}$$

$$S(r, t) = -\frac{2t}{\pi F} \sum_{j=1}^{3} \int_0^\infty \alpha g_j \gamma_j \sum_{i=1}^{3} \frac{P_i(\alpha, t) Q_{i,j}(\alpha)}{|\mathbf{C}(\alpha)|} I_0(\gamma_j' \alpha r) \, \mathrm{d}\alpha, \tag{43}$$

$$F = \sum_{j=1}^{3} g_j d_j, \tag{44}$$

$$g_j = c_{13} a_j - c_{33} + e_{33} b_j \quad (j = 1, 2, 3). \tag{45}$$

In Eq. 42, K and E are complete elliptic integrals of the first and second kind, respectively. Note that $R(r, t)$ denotes the singular part, whereas $S(r, t)$ is regular. Then, the first of Eq. 14 yields

$$\int_c^a \psi(t) \{R(r, t) + S(r, t)\} \, \mathrm{d}t = -\frac{\pi}{2F} \sigma_\infty, \quad c < r < a. \tag{46}$$

Prior to the numerical solution of (46), it is normalized by introducing

$$r = \frac{a - c}{2} v + \frac{a + c}{2}, \quad t = \frac{a - c}{2} w + \frac{a + c}{2}, \tag{47}$$

$$\psi(t) = -\frac{\pi \sigma_\infty}{(a - c) F} \frac{\Psi(w)}{(1 - w^2)^{1/2}}. \tag{48}$$

If we now substitute (47) and (48) in (46) and (38), we get

$$\int_{-1}^{1} \frac{1}{(1 - w^2)^{1/2}} \{R^*(v, w) + S^*(v, w)\} \Psi(w) \, \mathrm{d}w = 1, \quad -1 < v < 1, \tag{49}$$

$$\int_{-1}^{1} \frac{1}{(1 - w^2)^{1/2}} \Psi(w) \, \mathrm{d}w = 0, \tag{50}$$

where

$$R^*(v, w) = R(r, t), \tag{51}$$

$$S^*(v, w) = S(r, t). \tag{52}$$

Using the Lobatto–Chebyshev method [14], we may cast Eqs. 49 and 50 into the matrix form as

$$\sum_{k=1}^{N} W_k\{R^*(v_i,w_k)+S^*(v_i,w_k)\}\Psi(w_k)=1 \quad (i=1,\ldots,N-1), \tag{53}$$

$$\sum_{k=1}^{N} W_k\Psi(w_k)=0, \tag{54}$$

where

$$v_i=\cos\left(\frac{i-1/2}{N-1}\pi\right) \quad (i=1,\ldots N-1), \tag{55}$$

$$w_k=\cos\left(\frac{k-1}{N-1}\pi\right) \quad (k=1,\ldots,N), \tag{56}$$

$$W_k=\frac{\pi}{N-1} \quad (k=2,\ldots,N-1), \quad W_k=\frac{\pi}{2(N-1)} \quad (k=1,N). \tag{57}$$

For $c=0$ [11], the integral in (49) can be evaluated by using the Gaussian quadrature formula.

The stress-intensity factor k_1^i at the inner tip of the flat annular crack is obtained as

$$\begin{aligned} k_1^i &= \lim_{r\to c^-}\{2(c-r)\}^{1/2}\sigma_{zz}(r,0) \\ &= \sigma_\infty\left(\frac{2}{a-c}\right)^{1/2}\Psi(-1). \end{aligned} \tag{58}$$

The stress-intensity factor k_1^o at the outer tip of the crack is

$$\begin{aligned} k_1^o &= \lim_{r\to a^+}\{2(r-a)\}^{1/2}\sigma_{zz}(r,0) \\ &= -\sigma_\infty\left(\frac{2}{a-c}\right)^{1/2}\Psi(1). \end{aligned} \tag{59}$$

Also obtained are expressions for the energy-release rate and energy-density factor:

$$G^\delta=\frac{\pi}{2F^2}\left(F\sum_{j=1}^{3}\frac{d_j}{\gamma_j}-\sum_{j=1}^{3}h_jd_j\sum_{j=1}^{3}\frac{b_jd_j}{\gamma_j}\right)(k_1^\delta)^2 \quad (\delta=i,o), \tag{60}$$

$$S^\delta=(a_M^\delta+a_E^\delta)(k_1^\delta)^2 \quad (\delta=i,o), \tag{61}$$

where

$$\begin{aligned} a_M^\delta=\frac{1}{8F^2}\Bigg\{&\sum_{j=1}^{3}m_jd_jR_j^c(\theta_1^\delta)\sum_{j=1}^{3}a_jd_jR_j^c(\theta_1^\delta)+\sum_{j=1}^{3}\frac{f_jd_j}{\gamma_j}R_j^s(\theta_1^\delta)\sum_{j=1}^{3}\frac{d_j(a_j\gamma_j^2+1)}{\gamma_j}R_j^s(\theta_1^\delta) \\ &-\sum_{j=1}^{3}g_jd_jR_j^c(\theta_1^\delta)\sum_{j=1}^{3}d_jR_j^c(\theta_1^\delta)\Bigg\}, \end{aligned} \tag{62}$$

$$a_E^\delta=\frac{1}{8F^2}\left\{\sum_{j=1}^{3}\frac{n_j}{\gamma_j}d_jR_j^s(\theta_1^\delta)\sum_{j=1}^{3}\frac{b_jd_j}{\gamma_j}R_j^s(\theta_1^\delta)-\sum_{j=1}^{3}h_jd_jR_j^c(\theta_1^\delta)\sum_{j=1}^{3}b_jd_jR_j^c(\theta_1^\delta)\right\}, \tag{63}$$

and

$$R_j^c(\theta_1^\delta) = \left\{ \frac{(\cos^2\theta_1^\delta + \gamma_j^2 \sin^2\theta_1^\delta)^{1/2} + \cos\theta_1^\delta}{\cos^2\theta_1^\delta + \gamma_j^2 \sin^2\theta_1^\delta} \right\}^{1/2},$$
$$R_j^s(\theta_1^\delta) = -\left\{ \frac{(\cos^2\theta_1^\delta + \gamma_j^2 \sin^2\theta_1^\delta)^{1/2} - \cos\theta_1^\delta}{\cos^2\theta_1^\delta + \gamma_j^2 \sin^2\theta_1^\delta} \right\}^{1/2} \qquad (\delta = i, o), \tag{64}$$

$$\theta_1^i = \tan^{-1}\left(\frac{z}{c - r_1^i}\right), \quad r_1^i = \{(c-r)^2 + z^2\}^{1/2}, \tag{65}$$

$$\theta_1^o = \tan^{-1}\left(\frac{z}{r_1^o - a}\right), \quad r_1^o = \{(r-a)^2 + z^2\}^{1/2}. \tag{66}$$

4 Numerical results and discussion

To examine the effect of electroelastic interactions on the stress-intensity factor, energy-release rate and energy-density factor for a flat annular permeable crack, the solution of the singular integral equation (49) governing $\Psi(w)$ has been computed numerically by the use of Lobatto–Chebyshev method. Once this has been done, k_1^δ, G^δ and $S^\delta(\delta = i, o)$ can be found from (58–61). The piezoelectric fibers are assumed to be the commercially available PZTs P-7 (Murata Manufacturing Co., Ltd., Japan) and C-91 (Fuji Ceramics Co., Ltd., Japan). The material properties are listed in Table 1. The matrix is epoxy, epoxy with 30.5% glass beads [1], or aluminum [15]. The Young's modulus E and Poisson's ratio ν are listed in Table 2.

Figure 2 shows the normalized stress-intensity factors $\pi k_1^\delta / 2\sigma_0 a^{1/2} (\delta = i, o)$ versus inner-crack-radius to outer-crack-radius ratio c/a for a P-7-epoxy composite with $a/b = 0.9$ under the normalized electric field $e_1 E_\infty / \sigma_0 = 0$. The normalized stress-intensity factors $\pi k_1^\delta / 2\sigma_0 a^{1/2}$ of a free-surface P-7 fiber under $e_1 E_\infty / \sigma_0 = 0$ is included for comparison purposes. The stress-intensity factor of the P-7-epoxy composite remains smaller than that of the P-7 fiber. It may also be seen that k_1^i is larger than k_1^o. An increase in the stress-intensity factor is observed with a decrease of c/a. The normalized stress-intensity factor $\pi k_1^o / 2\sigma_0 a^{1/2}$ tends to the result for a penny-shaped crack [11] as $c/a \to 0$. When $(a - c)/a \to 0$, both $\pi k_1^i / 2\sigma_0 a^{1/2}$ and $\pi k_1^o / 2\sigma_0 a^{1/2}$ approach the normalized stress-intensity factor for a Griffith crack of length $a - c$ in the plane-strain state. Results are presented in the form of plots for the normalized stress-intensity

Table 1 Material properties of piezoelectric ceramics P-7 and C-91

	Elastic stiffnesses ($\times 10^{10}$ N/m^2)					Piezoelectric coefficients (C/m^2)			Dielectric constants ($\times 10^{-10}$ C/Vm)	
	c_{11}	c_{33}	c_{44}	c_{12}	c_{13}	e_{31}	e_{33}	e_{15}	ϵ_{11}	ϵ_{33}
P-7	13.0	11.9	2.5	8.3	8.3	−10.3	14.7	13.5	171	186
C-91	12.0	7.7	7.7	11.4	2.4	−17.3	21.2	20.2	226	235

Table 2 Material properties of matrix

	Young's modulus E ($\times 10^{10}$ N/m^2)	Poisson's ratio ν
Epoxy	0.300	0.35
Epoxy+30.5% glass beads	0.440	0.36
Aluminum	7.0	0.33

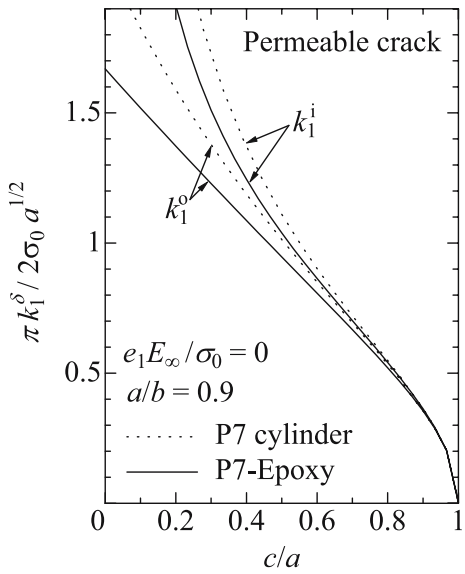

Fig. 2 Stress-intensity factor versus radius ratio c/a for $a/b = 0.9$

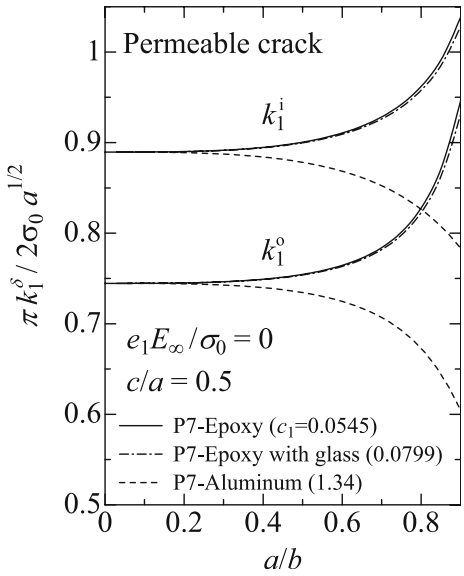

Fig. 3 Stress-intensity factor versus a/b for $c/a = 0.5$

factors $\pi k_1^\delta/2\sigma_0 a^{1/2} (\delta = i, o)$ as a function of a/b for some P-7 fiber composites with $c/a = 0.5$ under $e_1E_\infty/\sigma_0 = 0$ in Fig. 3. The stress-intensity factors k_1^i and k_1^o are seen to increase with increasing a/b ratios for $c_1 < 1$ and to decrease with increasing values of a/b when $c_1 > 1$. In the limiting case of $b \to \infty$, the problem becomes one of an infinite piezoelectric medium with a flat annular crack. Thus, the solution can be easily evaluated numerically. From the first of Eq. 23 and Eqs. 58, 59, it is clear that the electric field E_∞ has an effect on the stress intensity factors k_1^i and k_1^o (not shown).

Figure 4 shows the dependence of the energy-release rate G^o/G_0^o at the outer tip of the crack on e_1E_∞/σ_0 for some piezoelectric composites with $a/b = 0.9$ and $c/a = 0.5$ under uniform strain, where the results have been normalized by the values of the infinite PZTs without electric field, respectively. Also shown is the energy-density factor S^o/S_0^o. Comparing the results of G^o/G_0^o and S^o/S_0^o, we do not observe a difference. Application of a positive electric field to the piezoelectric fiber reduces the energy-release rate and energy-density factor, while a negative electric field causes them to increase. The matrix properties have a definite effect on the energy-release rate and energy-density factor. The energy-release rate and energy-density factor under uniform stress are independent of the electric field (no figure shown). Figure 5 shows similar results for the energy-release rate G^i/G_0^i and energy-density factor S^i/S_0^i at the inner tip of the crack.

5 Conclusions

The mode I fracture-mechanics parameters, such as stress intensity factor, energy-release rate and energy density factor are presented for a flat annular permeable crack in piezoelectric fiber composites.

Based on the results of this study, the following conclusions may be drawn:

- The fracture-mechanics parameters of piezoelectric fiber composites increase or decrease with increasing the inner-crack radius to outer-crack radius ratio, depending on the matrix-material properties.
- Since the surrounding matrix restricts the deformation of the piezoelectric fibers, the fracture-mechanics parameters of the piezoelectric fiber composites are smaller than those for piezoelectric fibers.

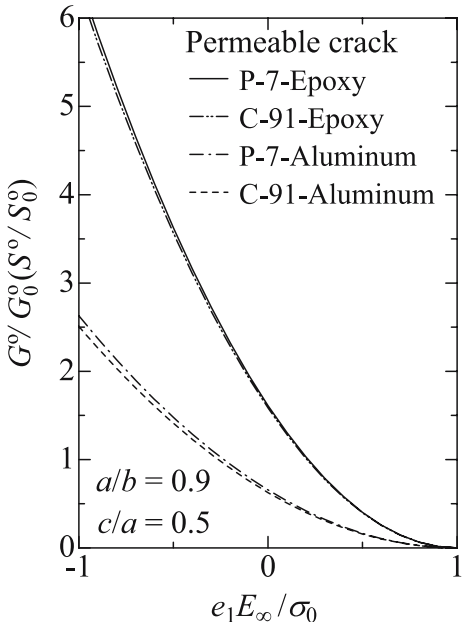

Fig. 4 Energy-release rate at outer tip of crack versus electric field ($a/b = 0.9, c/a = 0.5$)

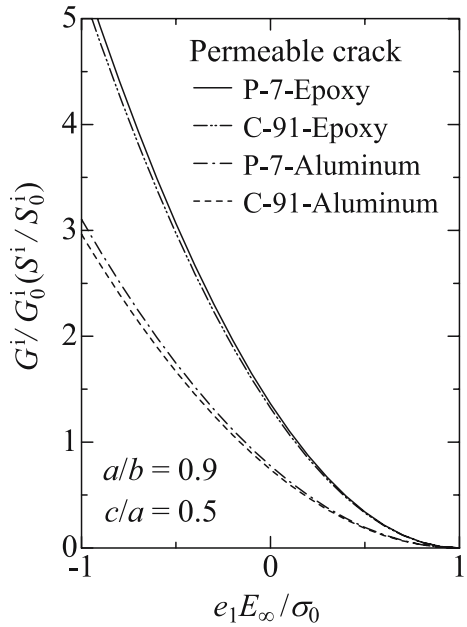

Fig. 5 Energy-release rate at inner tip of crack versus electric field ($a/b = 0.9, c/a = 0.5$)

- The fracture mechanics parameters of the inner tip of the flat annular crack are always larger than those of the outer crack tip.
- A positive electric field decreases the fracture-mechanics parameters under an applied uniform strain, while a negative one has the opposite effect.

The results of this work provide a basis for assessing the operating life of piezoelectric fiber composites resulting from a pre-existing three-dimensional crack. Although this piezoelectric crack problem has a simple geometry, the current analysis can be easily extended to investigate the fracture-mechanics parameters in other types of composite materials (e.g. cracked piezoelectric composites with fiber coating, composites with a completely broken piezoelectric fiber, etc.). Work in this area is currently being pursued.

Acknowledgements The work was supported by the Ministry of Education, Culture, Sports, Science and Technology of Japan under the Grant-in-Aid for Young Scientists (B).

Appendix 1

To solve the differential equations (8) and (9), we use integral transforms. Applying the Hankel transform with respect to r to (8) and (9), we find

$$\begin{bmatrix} c_{11}\alpha^2 - c_{44}\dfrac{\mathrm{d}^2}{\mathrm{d}z^2} & (c_{13}+c_{44})\alpha\dfrac{\mathrm{d}}{\mathrm{d}z} & (e_{31}+e_{15})\alpha\dfrac{\mathrm{d}}{\mathrm{d}z} \\ (c_{13}+c_{44})\alpha\dfrac{\mathrm{d}}{\mathrm{d}z} & c_{33}\dfrac{\mathrm{d}^2}{\mathrm{d}z^2} - c_{44}\alpha^2 & -e_{15}\alpha^2 + e_{33}\dfrac{\mathrm{d}^2}{\mathrm{d}z^2} \\ (e_{31}+e_{15})\alpha\dfrac{\mathrm{d}}{\mathrm{d}z} & -e_{15}\alpha^2 + e_{33}\dfrac{\mathrm{d}^2}{\mathrm{d}z^2} & \epsilon_{11}\alpha^2 - \epsilon_{33}\dfrac{\mathrm{d}^2}{\mathrm{d}z^2} \end{bmatrix} \begin{pmatrix} \bar{u}_r \\ \bar{u}_z \\ \bar{\phi} \end{pmatrix} = 0, \tag{67}$$

where

$$\begin{aligned}\bar{u}_r(\alpha,z) &= \int_0^\infty r u_r(r,z)J_1(\alpha r)\mathrm{d}r,\\ \bar{u}_z(\alpha,z) &= \int_0^\infty r u_z(r,z)J_0(\alpha r)\mathrm{d}r,\\ \bar{\phi}(\alpha,z) &= \int_0^\infty r\phi(r,z)J_0(\alpha r)\mathrm{d}r.\end{aligned} \tag{68}$$

There are three ordinary equations with three unknowns: hence, from standard methodology, a general exponential form, $\exp(-\gamma\alpha z)$, of the solution for the transformed principal variables results. The parameter γ must satisfy the following characteristic equations:

$$a_0\gamma^6 + b_0\gamma^4 + c_0\gamma^2 + d_0 = 0, \tag{69}$$

where

$$\begin{aligned}a_0 &= c_{44}(c_{33}\epsilon_{33} + e_{33}^2),\\ b_0 &= -2c_{44}e_{15}e_{33} - c_{11}e_{33}^2 - c_{33}(c_{44}\epsilon_{11} + c_{11}\epsilon_{33}) + \epsilon_{33}(c_{13}+c_{44})^2\\ &\quad +2e_{33}(c_{13}+c_{44})(e_{31}+e_{15}) - c_{44}^2\epsilon_{33} - c_{33}(e_{31}+e_{15})^2,\\ c_0 &= 2c_{11}e_{15}e_{33} + c_{44}e_{15}^2 + c_{11}(c_{33}\epsilon_{11} + c_{44}\epsilon_{33}) - \epsilon_{11}(c_{13}+c_{44})^2\\ &\quad -2e_{15}(c_{13}+c_{44})(e_{31}+e_{15}) + c_{44}^2\epsilon_{11} + c_{44}(e_{31}+e_{15})^2,\\ d_0 &= -c_{11}(c_{44}\epsilon_{11} + e_{15}^2).\end{aligned} \tag{70}$$

The solutions of (67) may then be expressed as

$$\begin{aligned}\bar{u}_r &= \frac{2}{\pi\alpha}\sum_{j=1}^{3} a_j A_j(\alpha)\exp(-\gamma_j\alpha z),\\ \bar{u}_z &= \frac{2}{\pi\alpha}\sum_{j=1}^{3} \frac{1}{\gamma_j} A_j(\alpha)\exp(-\gamma_j\alpha z),\\ \bar{\phi} &= -\frac{2}{\pi\alpha}\sum_{j=1}^{3} \frac{b_j}{\gamma_j} A_j(\alpha)\exp(-\gamma_j\alpha z),\end{aligned} \tag{71}$$

where γ_j^2 $(j=1,2,3)$ are the roots of (69), and a_j, b_j $(j=1,2,3)$ stand for the following abbreviations:

$$a_j = \frac{(e_{31}+e_{15})(c_{33}\gamma_j^2 - c_{44}) - (c_{13}+c_{44})(e_{33}\gamma_j^2 - e_{15})}{(c_{44}\gamma_j^2 - c_{11})(e_{33}\gamma_j^2 - e_{15}) + (c_{13}+c_{44})(e_{31}+e_{15})\gamma_j^2}, \tag{72}$$

$$b_j = \frac{(c_{44}\gamma_j^2 - c_{11})a_j + (c_{13}+c_{44})}{e_{31}+e_{15}}. \tag{73}$$

Similarly, one can take the Fourier transforms of (8) and (9) relative to z. The results are

$$\begin{bmatrix} r_{11} & r_{21} & r_{13}\\ r_{21} & r_{22} & r_{23}\\ r_{31} & r_{32} & r_{33}\end{bmatrix}\begin{pmatrix}\bar{u}_r\\ \bar{u}_{z,r}\\ \bar{\phi}_{,r}\end{pmatrix} = 0, \tag{74}$$

where

$$
\begin{aligned}
r_{11} &= c_{11}\left(\frac{\mathrm{d}^2}{\mathrm{d}r^2}+\frac{1}{r}\frac{\mathrm{d}}{\mathrm{d}r}-\frac{1}{r^2}\right)-c_{44}\alpha^2,\\
r_{12} &= -\mathrm{i}(c_{13}+c_{44})\alpha,\\
r_{13} &= -\mathrm{i}(e_{31}+e_{15})\alpha,\\
r_{21} &= -\mathrm{i}(c_{13}+c_{44})\alpha\left(\frac{\mathrm{d}^2}{\mathrm{d}r^2}+\frac{1}{r}\frac{\mathrm{d}}{\mathrm{d}r}-\frac{1}{r^2}\right),\\
r_{22} &= -c_{33}\alpha^2+c_{44}\left(\frac{\mathrm{d}^2}{\mathrm{d}r^2}+\frac{1}{r}\frac{\mathrm{d}}{\mathrm{d}r}-\frac{1}{r^2}\right),\\
r_{23} &= e_{15}\left(\frac{\mathrm{d}^2}{\mathrm{d}r^2}+\frac{1}{r}\frac{\mathrm{d}}{\mathrm{d}r}-\frac{1}{r^2}\right)-e_{33}\alpha^2,\\
r_{31} &= -\mathrm{i}(e_{31}+e_{15})\alpha\left(\frac{\mathrm{d}^2}{\mathrm{d}r^2}+\frac{1}{r}\frac{\mathrm{d}}{\mathrm{d}r}-\frac{1}{r^2}\right),\\
r_{32} &= e_{15}\left(\frac{\mathrm{d}^2}{\mathrm{d}r^2}+\frac{1}{r}\frac{\mathrm{d}}{\mathrm{d}r}-\frac{1}{r^2}\right)-e_{33}\alpha^2,\\
r_{33} &= -\epsilon_{11}\left(\frac{\mathrm{d}^2}{\mathrm{d}r^2}+\frac{1}{r}\frac{\mathrm{d}}{\mathrm{d}r}-\frac{1}{r^2}\right)+\epsilon_{33}\alpha^2,
\end{aligned}
\tag{75}
$$

and

$$
\begin{aligned}
\bar{u}_r(\alpha,r) &= \int_{-\infty}^{\infty} u_r(r,z)\exp(\mathrm{i}\alpha z)\mathrm{d}z,\\
\bar{u}_z(\alpha,r) &= \int_{-\infty}^{\infty} u_z(r,z)\exp(\mathrm{i}\alpha z)\mathrm{d}z,\\
\bar{\phi}(\alpha,r) &= \int_{-\infty}^{\infty} \phi(r,z)\exp(\mathrm{i}\alpha z)\mathrm{d}z.
\end{aligned}
\tag{76}
$$

The solutions are

$$
\begin{aligned}
\bar{u}_r &= \frac{2}{\alpha}\sum_{j=1}^{3} a_j' B_j(\alpha) I_1(\gamma_j'\alpha r),\\
\bar{u}_z &= \frac{2}{\alpha}\sum_{j=1}^{3} \frac{1}{\gamma_j'} B_j(\alpha) I_0(\gamma_j'\alpha r),\\
\bar{\phi} &= -\frac{2}{\alpha}\sum_{j=1}^{3} \frac{b_j'}{\gamma_j'} B_j(\alpha) I_0(\gamma_j'\alpha r),
\end{aligned}
\tag{77}
$$

where

$$
\gamma_j'^2 = \frac{1}{\gamma_j^2}, \tag{78}
$$

$$
a_j' = -a_j\gamma_j^2, \tag{79}
$$

$$
b_j' = -b_j. \tag{80}
$$

After considering the symmetry and far-field conditions, superposition of the solutions [(71) and (77)] yields (26) and (27). A similar procedure may be employed to derive the displacements for the outside elastic material and hence Eq. 28 can be obtained.

Appendix 2

$P_i(\alpha,t)$ $(i=1,\ldots,5)$ and $\mathbf{C}(\alpha)$ in Eq. 40 are given by

$$
\begin{aligned}
P_1(\alpha,t) &= \sum_{j=1}^{3} a_j d_j \gamma_j' I_1(\gamma_j'\alpha t) K_1(\gamma_j'\alpha b),\\
P_2(\alpha,t) &= \sum_{j=1}^{3} d_j \gamma_j'^2 I_1(\gamma_j'\alpha t) K_0(\gamma_j'\alpha b),\\
P_3(\alpha,t) &= \sum_{j=1}^{3} d_j I_1(\gamma_j'\alpha t)\left\{ m_j \gamma_j'^2 K_0(\gamma_j'\alpha b) - \frac{1}{\alpha b}(c_{12}-c_{11}) a_j \gamma_j' K_1(\gamma_j'\alpha b)\right\},\\
P_4(\alpha,t) &= -\sum_{j=1}^{3} d_j f_j \gamma_j'^3 I_1(\gamma_j'\alpha t) K_1(\gamma_j'\alpha b),\\
P_5(\alpha,t) &= -\sum_{j=1}^{3} d_j n_j \gamma_j'^3 I_1(\gamma_j'\alpha t) K_1(\gamma_j'\alpha b),
\end{aligned}
\tag{81}
$$

and

$$
\mathbf{C}(\alpha) = \begin{bmatrix}
c_{1,1}(\alpha) & c_{1,2}(\alpha) & c_{1,3}(\alpha) & c_{1,4}(\alpha) & c_{1,5}(\alpha)\\
c_{2,1}(\alpha) & c_{2,2}(\alpha) & c_{2,3}(\alpha) & c_{2,4}(\alpha) & c_{2,5}(\alpha)\\
c_{3,1}(\alpha) & c_{3,2}(\alpha) & c_{3,3}(\alpha) & c_{3,4}(\alpha) & c_{3,5}(\alpha)\\
c_{4,1}(\alpha) & c_{4,2}(\alpha) & c_{4,3}(\alpha) & c_{4,4}(\alpha) & c_{4,5}(\alpha)\\
c_{5,1}(\alpha) & c_{5,2}(\alpha) & c_{5,3}(\alpha) & c_{5,4}(\alpha) & c_{5,5}(\alpha)
\end{bmatrix}.
\tag{82}
$$

In (82), the elements $c_{i,j}(\alpha)$ are

$$
\left.
\begin{aligned}
c_{1,j}(\alpha) &= a_j' I_1(\gamma_j'\alpha b),\\
c_{2,j}(\alpha) &= \gamma_j I_0(\gamma_j'\alpha b),\\
c_{3,j}(\alpha) &= m_j\gamma_j I_0(\gamma_j'\alpha b) - \frac{1}{\alpha b}(c_{12}-c_{11}) a_j' I_1(\gamma_j'\alpha b),\\
c_{4,j}(\alpha) &= f_j I_1(\gamma_j'\alpha b),\\
c_{5,j}(\alpha) &= n_j I_1(\gamma_j'\alpha b),
\end{aligned}
\right\} \quad (j=1,2,3),
\tag{83}
$$

$$
\left.
\begin{aligned}
c_{1,4}(\alpha) &= K_1(\alpha b),\\
c_{2,4}(\alpha) &= K_0(\alpha b),\\
c_{3,4}(\alpha) &= \frac{2\mu}{\alpha b}[\alpha b K_0(\alpha b) + K_1(\alpha b)],\\
c_{4,4}(\alpha) &= -2\mu K_1(\alpha b),\\
c_{5,4}(\alpha) &= 0,
\end{aligned}
\right\}
\tag{84}
$$

$$
\left.
\begin{aligned}
c_{1,5}(\alpha) &= -4(1-\nu)K_1(\alpha b) - \alpha b K_0(\alpha b),\\
c_{2,5}(\alpha) &= -\alpha b K_1(\alpha b),\\
c_{3,5}(\alpha) &= -\frac{2\mu}{\alpha b}\big[(4-4\nu+\alpha^2 b^2)K_1(\alpha b) + (3-2\nu)\alpha b K_0(\alpha b)\big],\\
c_{4,5}(\alpha) &= 2\mu[(2-2\nu)K_1(\alpha b) + \alpha b K_0(\alpha b)],\\
c_{5,5}(\alpha) &= 0,
\end{aligned}
\right\}
\tag{85}
$$

where

$$
m_j = c_{11}a_j - c_{13} + e_{31}b_j \quad (j=1,2,3),
\tag{86}
$$

$$
n_j = e_{15}(a_j\gamma_j^2 + 1) - \epsilon_{11}b_j \quad (j=1,2,3).
\tag{87}
$$

In (40) $|\mathbf{C}(\alpha)|$ is the determinant of the square matrix $\mathbf{C}(\alpha)$ and $Q_{i,j}(\alpha)$ are the cofactors of the elements $c_{i,j}(\alpha)$.

References

1. Agbossou A, Richard C, Vigier Y (2003) Segmented piezoelectric fiber composite for vibration control: fabricating and modeling of electromechanical properties. Comp Sci Technol 63:871–881
2. Wang DY, Li K, Chan HLW (2004) High frequency 1-3 composite transducer fabricated using sol-gel derived lead-free BNBT fibers. Sensors Actuat A114:1–6
3. Barbezat M, Brunner AJ, Flueler P, Huber C, Kornmann X (2004) Acoustic emission sensor properties of active fibre composite elements compared with commercial acoustic emission sensors. Sensors Actuat A114:13–20
4. Schneider GA, Heyer V (1999) Influence of the electric field on Vickers indentation crack growth in $BaTiO_3$. J Eur Ceram Soc 19:1299–1306
5. Shindo Y, Narita F, Horiguchi K, Magara Y, Yoshida M (2003) Electric fracture and polarization switching properties of piezoelectric ceramic PZT studied by the modified small punch test. Acta Mater 51:4773–4782
6. Zhang TY, Gao CF (2004) Fracture behaviors of piezoelectric materials. Theor Appl Fract Mech 41:339–379
7. Shindo Y, Narita F, Mikami M (2005) Double torsion testing and finite element analysis for determining the electric fracture properties of piezoelectric ceramics. J App Phys 97:114109
8. McMeeking RM (1999) Crack tip energy release rate for a piezoelectric compact tension specimen. Eng Fract Mech 64:217–244
9. Chen W, Lynch CS (1999) Finite element analysis of cracks in ferroelectric ceramic materials. Eng Fract Mech 64:539–562
10. Lin S, Narita F, Shindo Y (2003) Comparison of energy release rate and energy density criteria for a piezoelectric layered composite with a crack normal to interface. Theor Appl Fract Mech 39:229–243.
11. Lin S, Narita F, Shindo Y (2003) Electroelastic analysis of a piezoelectric cylindrical fiber with a penny-shaped crack embedded in a matrix. Int J Solids Struct 40:5157–5174
12. Narita F, Shindo Y, Horiguchi K (2003) Electroelastic fracture mechanics of piezoelectric ceramics. In: Shindo Y (ed) Mechanics of electromagnetic material systems and structures. WIT Press, pp 89–101
13. Mindlin RD (1974) Equations of high frequency vibrations of thermopiezoelectric crystal plates. Int J Solids Struct 10:625–637
14. Theocaris PS, Ioakimidis NI (1979) Stress intensity factor as crack tips near boundaries or geometrical discontinuities. Int J Fract 15:419–428
15. Dai HL, Wang X (2006) Stress wave propagation in piezoelectric fiber reinfored laminated composites subjected to thermal shock. Comp Struct 74:51–62